

Geometry of tilt (in)variance in scanned oblique plane microscopy

Manish Kumar¹ and Yevgenia Kozorovitskiy^{1,*}

¹Department of Neurobiology, Northwestern University
**Yevgenia.Kozorovitskiy@northwestern.edu*

January 11, 2020

Tilt invariant scanning of light-sheet is crucial for distortion free 3D imaging in scanned oblique plane microscopy. In this Letter, we evaluate whether a plane mirror scanner can provide absolutely tilt invariant lateral scanning and imaging. Here, we derive the geometrical relationship for tilt variance of scanned oblique beams and propose experimental strategy for its verification.

1 Introduction

Oblique plane microscopy (OPM) provides a useful configuration for light-sheet microscopy using a single front facing microscope objective based setup [1]. In its original configuration, the microscope performs 3D imaging by axial scanning of the light-sheet [2], achieved by a piezo mounted microscope objective. Remote objective movement results in a tilt invariant scan of the generated light-sheet, making 3D reconstruction simple and free of geometrical distortions. Recently, new scan configurations inspired by OPM have been implemented for more convenient, lateral scanning of the generated light-sheet. A polygon scan mirror based reflective arrangement and a transmission window based refractive arrangement have been recently introduced [3, 4]. While the refractive window based solution is tilt invariant for small scan ranges, the polygon mirror based arrangement suffers from large tilt variance during scanning.

We have recently used a planar scanner, with its rotation axis at the intersection of the back focal plane (BFP) and the principal axis of the scan lens, to resolve the tilt variance problem for both scanned illumination and descanned signal rays [5]. There has been a steady rise in the popularity of this particular scanned oblique plane illumination (SOPi) geometry for lateral scanning OPM style techniques [6, 7, 8, 9]. Therefore, it is essential to understand the underlying scan principles and limitations in oblique plane microscopy. In this Letter, we perform a detailed geometrical analysis of this scan arrangement. We derive a relationship for evaluating tilt variance in a light-sheet scanned through previously described SOPi geometry. We also propose an experiment to measure the actual variation in the tilt of an oblique beam.

2 Geometrical derivation

An optical lens is well known to behave as an optical Fourier transforming element [10]. A point source placed on the BFP of an ideal thin lens (optical aberration free) provides a set of collimated optical rays. As shown in Fig. 1(a), a point source offset by distance y leads to collimated optical rays with tilt angle α . In other words, if an optical ray emerges from a lens with a known tilt α , it can be uniquely associated with an offset point R on the BFP which is $y = f \times \tan(\alpha)$ distance apart from the optical axis, where f is the focal length of the lens. This Fourier transforming property of an optical lens can be extended to describe an ideal tilt invariant scan as shown in Fig. 1(b). If a rotary scanner, e.g. a galvanometer mounted planar mirror, is placed with its rotation axis at R (on the

BFP) and a laser beam hits the rotation axis of the mirror, then the reflected beam remains pivoted at R during the scan. This implies that the optical beam maintains a constant tilt angle after passing through the optical lens. This tilt angle

$$\alpha = \tan^{-1} \left(\frac{y}{f} \right) \quad (1)$$

can be easily changed by shifting the scanner and, hence, the optical beam pivot point R along the BFP.

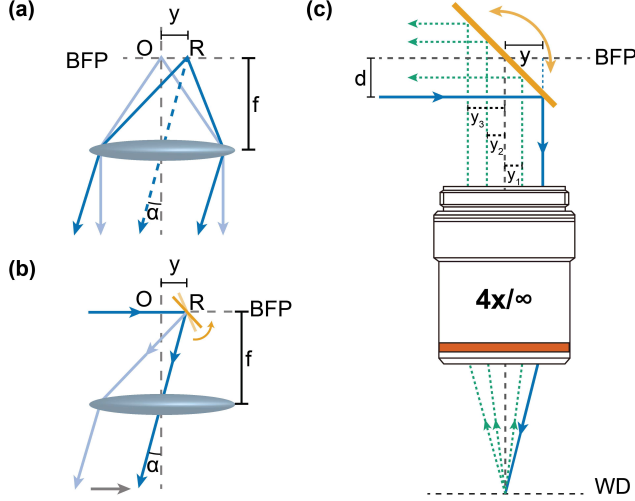


Fig. 1: Lens as an optical Fourier transforming element for tilt invariant scan. BFP: back focal plane; WD: working distance.

The geometry shown in Fig. 1(b) provides an absolutely tilt invariant scanned oblique illumination beam. However, oblique plane microscopy also requires consideration of the signal rays, arising due to optical scattering or emitted fluorescence from the sample. Since signal rays in the microscope are not confined to a particular tilt angle, we need an optical scanner which provides tilt invariant scanning for a wide range of beam offsets. Figure 1(c) shows the optimal SOPi arrangement under consideration. An infinity corrected microscope objective serves as a Fourier transforming scan lens, and a plane mirror with its rotation axis at the intersection of the BFP and the principal axis operates as a scanner. A beam (blue) with offset y forms an oblique illumination beam, and signal optical rays (green dotted) emerge at various tilt angles, where each tilt angle corresponds to a unique offset value y_1, y_2, y_3 , etc. What remains to be determined is how the beam offset and therefore tilt angle of the optical rays change during scanning. Tilt variance in oblique optical beam would lead to distorted 3D scan of the sample, while beam offset dependent tilt variance would cause additional spherical aberration [11].

Next, we derive the relationship for scan dynamics of an optical beam in the geometry represented in Fig. 1(c). For a generalized approach, we consider scan geometry where the rotation axis of the scanner O is offset by d_y and d_z lengths along y and z axis, respectively. Figure 2 shows the magnified view of this arrangement. OL and KL represent the horizontal and vertical offsets of scanner rotation axis from the intersection point of the principal axis and the BFP, respectively. Thus, $OL = d_y$ and $KL = d_z$. An optical ray MN is incident parallel to the BFP with an offset d from the scanner rotation axis O . This ray crosses the principal axis at M and hits the 45° tilted scan mirror (light orange) at P to get reflected vertically downwards along the z axis. When extended, the reflected beam meets the BFP at R . Thus, $ON \perp NP$, $NP \perp PR$, $KM = PR = d + d_z$, and $ON = LM = NP = d$. We now consider a new scanner position (dark orange) with the tilt angle $45^\circ + \theta$. Following the laws of reflection, the optical ray now hits the scanner at Q and is reflected, making an angle 2θ with the z axis. This reflected optical ray, when traced backwards, meets the BFP at S . T is the intersection point of both reflected rays where $\angle PTQ = \angle RTS = 2\theta$. For an ideal scanner geometry, R and S should overlap, leading to a constant offset and hence an absolutely tilt invariant scan. However, in practice, the gap RS dictates the error, or tilt variance, during the scan.

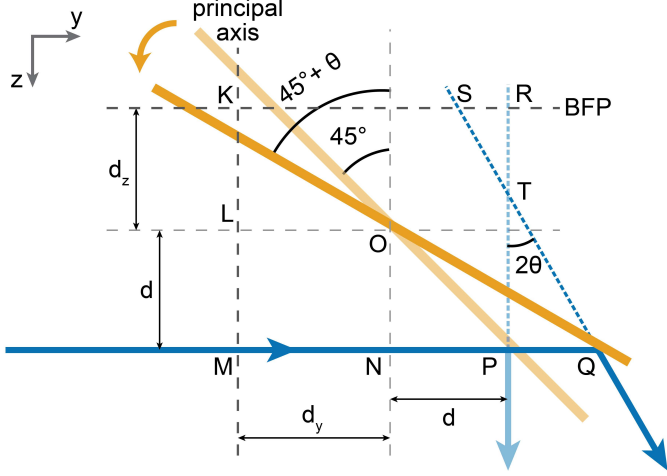


Fig. 2: Scan geometry for evaluation of tilt variance. BFP: back focal plane.

In ΔONQ we have $\tan(\angle NOQ) = NQ/ON = (NP + PQ)/ON = 1 + PQ/d$. Therefore, $PQ = d \times (\tan(\angle NOQ) - 1) = d \times (\tan(45^\circ + \theta) - 1) = d \times [(1 + \tan\theta)/(1 - \tan\theta) - 1]$.

Or,

$$PQ = \frac{2d \times \tan\theta}{1 - \tan\theta}. \quad (2)$$

In ΔTPQ we have $\tan(\angle PTQ) = PQ/PT = PQ/(PR - RT) = PQ/(d + d_z - RT)$. Therefore, $RT = d + d_z - PQ/\tan(\angle PTQ) = d + d_z - PQ/\tan(2\theta)$. Replacing PQ from Eq. 2 and expanding $\tan(2\theta)$ we get $RT = d + d_z - d \times (1 + \tan\theta)$

Or,

$$RT = d_z - d \times \tan\theta. \quad (3)$$

In ΔTRS we have $RS = RT \times \tan(\angle RTS) = (d_z - d \times \tan\theta) \times \tan(2\theta)$, where we replaced RT from Eq. 3. Now, expanding $\tan(2\theta)$ we get

$$RS = \frac{2d_z \times \tan\theta}{1 - \tan^2\theta} - \frac{2d \times \tan^2\theta}{1 - \tan^2\theta}. \quad (4)$$

Here, we can use RS to precisely calculate tilt variance in the oblique optical beam during scan. Usually, the practical value of scan angle θ is limited to $< 10^\circ$, implying that RS is smaller than d_z . If f is the focal length of the Fourier transforming lens, we can use Eq. 1 to express tilt variance in an optical beam as $\delta = |\alpha_0 - \alpha_\theta| = |\tan^{-1}(KR/f) - \tan^{-1}(KS/f)|$. Or,

$$\delta = \left| \tan^{-1} \left(\frac{d + d_y}{f} \right) - \tan^{-1} \left(\frac{d + d_y - RS}{f} \right) \right|. \quad (5)$$

In a practical case, Fourier transforming lenses have much longer focal length, compared to beam offsets and scanner position offsets (e.g. ref. [7] used $f = 100$ mm and offset $d = 3.54$ mm). Therefore, we have $(d + d_y)/f \ll 1$ and $(d + d_y - RS)/f \ll 1$ leading to the following small angle approximation $\delta \approx (d + d_y)/f - (d + d_y - RS)/f = RS/f$. Or, replacing RS from Eq. 4 we have

$$\delta \approx \left| \left(\frac{2d_z}{f} \times \frac{\tan\theta}{1 - \tan^2\theta} \right) - \left(\frac{2d}{f} \times \frac{\tan^2\theta}{1 - \tan^2\theta} \right) \right|, \quad (6)$$

where δ is in radians.

On a closer inspection of Eq. 4, it is clear that, $d_z = (d \times \tan\theta)$ makes RS zero, leading to an absolutely tilt invariant scan condition. However, this relationship cannot be satisfied for a wide range of θ unless $d_z = d = 0$. This happens when both the incident beam and the rotation axis of the scanner are aligned to the BFP, i.e. the ideal scan condition as shown in Fig. 1(b). If θ is restricted to small values, a nonzero d is allowed when d_z approaches zero. This optimized case is consistent with the

previously published geometry of SOPi, as shown in Fig. 1(c) [5, 7]. We can further conclude from the expression for RS that the scanning arrangement is very sensitive to any offset along the axial direction (d_z), but an offset along lateral direction (d_y) does not change tilt variance in the system. However, a non-zero d_y would change overall tilt of the oblique beam (see Eq. 1) and the off-axis placement of the scanner would make the imaging system asymmetric. Therefore, the most optimized scanning arrangement is one with $d_y = d_z = 0$. Here, the tilt variance expression from Eq. 5 becomes

$$\delta = \left| \tan^{-1} \left(\frac{d}{f} \right) - \tan^{-1} \left(\frac{d - RS}{f} \right) \right|, \quad (7)$$

which under large focal length and small offsets approximation reduces to $\delta \approx RS/f = (2d/f) \times [\tan^2 \theta / (1 - \tan^2 \theta)]$. Note that δ is in radians here. Considering an extreme example with a large scan angle $\theta = 10^\circ$, a large offset $d = 5$ mm, and $f = 100$ mm, we get tilt variance $\delta = 0.184^\circ$. This value of tilt variance is small for most practical purposes. In some cases tilt variance can get magnified and become significant, based on subsequent optical elements. For example, the SOPi setup in ref. [5] introduces $22.22 \times$ angular magnification. Thus, using the example case leads to the effective tilt variance in the sample volume of $\sim 4^\circ$.

3 Experimental design

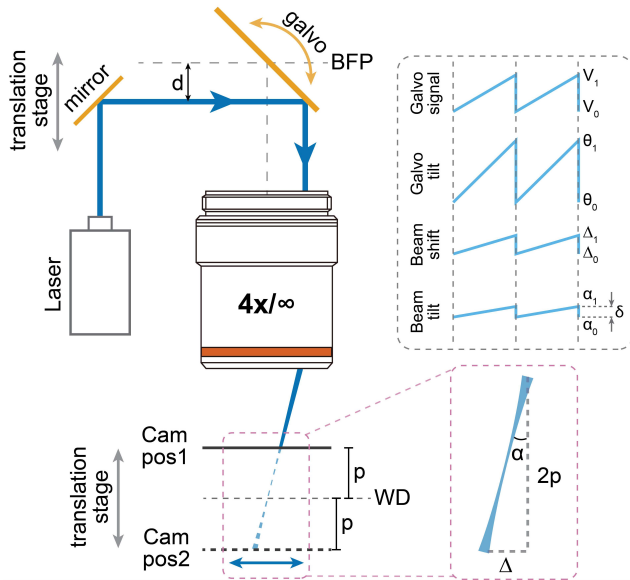


Fig. 3: Experimental setup for the evaluation of tilt variance.

Next, we propose an experimental validation of the derived tilt variance relationship *i.e.* Eq. 5. For this we needed a Fourier transforming lens, a plane mirror based scanner, and a way to measure the beam tilt α . The schematics of the setup are shown in Fig. 3. A low magnification, long working distance microscope objective ($4\times$) can be used as a Fourier transforming lens. The advantage of using a low magnification objective is that its BFP lies outside the body of the objective and is therefore easily accessible. A galvanometer mounted plane mirror serves as the scanner. The galvo scanner should be carefully aligned to match its rotation axis to the BFP. A visible light laser can be used for alignment and the experiment. During experiment, the laser beam is reflected towards the galvo scanner using a mirror mounted on a translation stage, to vary the offset d of the incident beam. Another translation stage holds a camera for measuring the outgoing beam tilt α . As shown in Fig. 3, the camera captures beam position at two predefined locations $\pm p$ distance away from the WD of the microscope objective, leading to an easy calculation of the beam tilt

$$\alpha = \tan^{-1} \left(\frac{\Delta}{2p} \right), \quad (8)$$

where Δ is the shift between beam positions as measured on camera sensor surfaces and $2p$ is the gap between camera sensor positions (see inset Fig. 3).

In conclusion, we have performed a geometrical analysis of scanned oblique plane microscopy, defined the optimal layout analytically, and proposed an experimental method for measuring tilt variance of specific objective and scanner arrangements. These results confirm that essentially tilt invariant scanning can be achieved by lateral scan implementations of OPM inspired systems, but highlight the importance of precise scanner positioning and alignment for tilt variance and aberration control.

Acknowledgements

This work was supported by NIH R01MH117111, Arnold and Mabel Beckman Foundation (Beckman Young Investigator Award), Kinship Foundation (Searle Scholar Award), and Rita Allen Foundation (Rita Allen Scholar Award).

References

- [1] C Dunsby. Optically sectioned imaging by oblique plane microscopy. *Optics express*, 16(25):20306–20316, 2008.
- [2] Sunil Kumar, Dean Wilding, Markus B Sikkel, Alexander R Lyon, Ken T MacLeod, and Chris Dunsby. High-speed 2d and 3d fluorescence microscopy of cardiac myocytes. *Optics express*, 19(15):13839–13847, 2011.
- [3] Matthew B Bouchard, Venkatakaushik Voleti, César S Mendes, Clay Lacefield, Wesley B Grueber, Richard S Mann, Randy M Bruno, and Elizabeth MC Hillman. Swept confocally-aligned planar excitation (scape) microscopy for high-speed volumetric imaging of behaving organisms. *Nature photonics*, 9(2):113, 2015.
- [4] Younghoon Shin, Dongmok Kim, and Hyuk-Sang Kwon. Oblique scanning 2-photon light-sheet fluorescence microscopy for rapid volumetric imaging. *Journal of biophotonics*, 11(5):e201700270, 2018.
- [5] Manish Kumar, Sandeep Kishore, Jordan Nasenbeny, David L McLean, and Yevgenia Kozorovitskiy. Integrated one-and two-photon scanned oblique plane illumination (sopi) microscopy for rapid volumetric imaging. *Optics express*, 26(10):13027–13041, 2018.
- [6] Bin Yang, Xingye Chen, Yina Wang, Siyu Feng, Veronica Pessino, Nico Stuurman, Nathan H Cho, Karen W Cheng, Samuel J Lord, Linfeng Xu, et al. Epi-illumination spim for volumetric imaging with high spatial-temporal resolution. *Nature methods*, 16(6):501, 2019.
- [7] Manish Kumar and Yevgenia Kozorovitskiy. Tilt-invariant scanned oblique plane illumination microscopy for large-scale volumetric imaging. *Optics letters*, 44(7):1706–1709, 2019.
- [8] Venkatakaushik Voleti, Kripa B Patel, Wenze Li, Citlali Perez Campos, Srinidhi Bharadwaj, Hang Yu, Caitlin Ford, Malte J Casper, Richard Wenwei Yan, Wenxuan Liang, et al. Real-time volumetric microscopy of *in vivo* dynamics and large-scale samples with scape 2.0. *Nature methods*, 16(10):1054–1062, 2019.
- [9] Maximilian Hoffmann and Benjamin Judkewitz. Diffractive oblique plane microscopy. *Optica*, 6(9):1166–1170, 2019.
- [10] Joseph W Goodman. *Introduction to Fourier optics*. Roberts and Company Publishers, 2005.
- [11] Robert Edward Fischer, Biljana Tadic-Galeb, and Paul R Yoder. *Optical System Design*. Spie Press Monograph. SPIE, 2008.